FATIGUE FAILURE FROM SUB-SURFACE DEFECTS IN A GAS TURBINE DISC ALLOY AT ELEVATED TEMPERATURE.

J. BYRNE*, N.Y.K. KAN*, I.W. HUSSEY** and G.F. HARRISON***
* Dept of Mechanical and Manufacturing Engineering
University of Portsmouth, Portsmouth, PO1 3DJ, U.K.
** Rolls-Royce plc., P.O.Box 31, Derby, DE24 8BJ, U.K.
*** Defence Research Agency, Farnborough, GU14 6TD, U.K.

ABSTRACT

The influence on fatigue life of sub-surface non-metallic inclusions has been studied in Waspaloy at 650°C under both load and effective strain control at a strain ratio of R=0.1. The specimens were shot peened to represent the component condition and to suppress free surface initiation. When compared with defect-free material in terms of total strain range, the presence of the defects reduced average cyclic lives by an order of magnitude. Use of a strain-life based model incorporating a mean stress effect, e.g., the Smith, Watson and Topper approach, could be used for life prediction, but this would require a large data base and/or large reserve factor on life. Alternatively, the use of the initial defect cluster size and LEFM shows a reasonable correlation in terms of the effective stress intensity range (ΔK_{eff}) and life, suggesting that confident safe life prediction requires the quantification of defect behaviour in terms of crack development and growth from the defects.

KEYWORDS

Fatigue; nickel base alloy; sub-surface defects; strain-life characterisation; crack growth threshold.

INTRODUCTION

The turbine disc is one of the most safety critical components in a gas turbine aero-engine (Jenkins and Pickard, 1989). If sub-surface defects are detected in a disc the whole batch may be scrapped, because of lack of understanding of their fatigue and fracture behaviour which can be strongly affected by defects (Denda et al, 1992).

Sub-surface defects, giving non-destructive testing (NDT) indications may be obtained in forged nickel-based alloy discs due to chemical heterogeneity known as "white spot" (Mitchell, 1986), ceramic inclusions and cracked inclusions. Such sub-surface defects may grow by fatigue or fatigue-creep at operating temperatures before the initiation of surface cracks when the disc surface has been shot peened and is under residual compressive stress

(Webster and Cunningham, 1993). The size, shape, orientation and distance below the surface of NDT indications will vary, influencing their fatigue crack growth (FCG) behaviour and the cyclic life (N_f).

The aim of this study was to understand and model how sub-surface defects affect the fatigue life of gas turbine discs. The initial hypothesis was that for a given stress/strain intensity level, above the threshold for fatigue crack growth, defects would crack during the first loading cycle and thereafter the fatigue cyclic life (N_f) would be entirely made up of crack propagation life, which could be characterised and modeled using fracture mechanics. This paper presents the results of the first part of the study, involving a strain-life comparison of defect-containing and plain specimens of Waspaloy at 650°C, together with a preliminary LEFM crack growth threshold assessment using ΔK_{th} for the initial defects.

MATERIAL DETAILS

The material studied was Waspaloy, with nominal composition of (wt%) 19 Cr, 13.5 Co, 4.25 Mo, 3 Ti, 1.25 Al, balance Ni. The nominal mechanical properties are given in Table 1.

Table 1. Mechanical Properties of Waspaloy at Room Temperature and 650°C

Mechanical Properties	RT°	650°C
Ultimate tensile strength	1,310 MPa	1,127 MPa
0.2% proof stress	927 MPa	809 MPa
Elongation	23%	21%
Reduction in area	25%	30%

Tensile push-pull specimens, 12×12 mm square in cross-section, were machined from disc forgings to include actual sub-surface defect indications detected by ultrasonic monitoring, approximately 0.5 mm below the surface, together with control defect-free samples. The specimen surfaces were shot-peened to represent the actual component condition and to inhibit free initiation at the surface.

EXPERIMENTAL DETAILS

All tests were conducted on an Instron 6027 twin screw electro-mechanical fatigue machine at 650°C and 0.25 Hz (trapezoidal) frequency in air under load and effective strain control, at a *strain* ratio of 0.1. Control monitoring of strain was achieved using an Instron quartz rod extensometer. Normally this is used with pointed conical end rods located on the specimen surface at surface indentations. However, for the shot peened surfaces, the indents were found to act as stress raisers and initiate cracks at these locations. An alternative method, without specimen indents, was developed to achieve effective strain control, using position control of the machine cross-head and a position-strain calibration. Throughout tests the actual strain range was monitored using wedge-end rods located on the specimen surfaces. No strain ratcheting was observed for the total strain ranges ($\Delta\varepsilon_t$) studied, up to 0.8%. A total of 10 defect containing specimens and 12 control (defect-free) specimens were tested to failure at $\Delta\varepsilon_t$ values between 0.3 and 0.8% to produce a strain-life fatigue curve for both conditions.

RESULTS

Strain-Life Analysis

A plot of strain amplitude ($\varepsilon_a = \frac{\Delta\varepsilon_t}{2}$) versus cycles to failure (N_f) is shown in Fig. 1. This shows a significant reduction in cyclic life for the defect indication specimens, apart from the three run-out results (arrowed) which are discussed in detail later. It should be noted that all the tests carried out were under all tensile strain conditions i.e. at a *strain* ratio of 0.1, with a tensile mean strain and stress, and that the simple basis for comparison used in Fig.1 needs modification.

The initial analysis involved the plotting of strain amplitude against the number of reversals to failure on logarithmic scales (Manson-Coffin, 1962). The material constants σ_f', ε_f', b and c are obtained from the intercept and the slope of the lines fitted through the data by regression analysis. In the absence of creep deformation the total strain amplitude consists only of time independent elastic and plastic strain amplitudes. Thus for a material showing straight "elastic" and "plastic" lines, the strain-life relationship may be represented by an equation of the form:

$$\frac{\Delta\varepsilon_t}{2} = \frac{\sigma_f'}{E}(2N_f)^b + \varepsilon_f'(2N_f)^c \qquad \text{.....(1)}$$

In order to estimate the constants in equation (1), the fatigue strength coefficient, σ_f', was assumed to be equal to the true fracture stress of the material under monotonic tensile loading, and the fatigue ductility coefficient, ε_f', was assumed to approximate to the elongation value to failure. This gives

$$\frac{\Delta\varepsilon_t}{2} = 6.57\times10^3(2N_f)^{-0.068} + 0.21(2N_f)^{-0.7208} \qquad \text{.....(2)}$$

which is compared with the test data in terms of strain *amplitude* ($\varepsilon_a = \frac{\Delta\varepsilon_t}{2}$) and reversals ($2N_f$) to failure, in Fig. 2. This shows a reasonable correlation with the control specimen failure lives.

When non-zero levels of mean stress are employed the strain-life behaviour may be correlated using the correction according to Morrow (1968), replacing the term σ_f' in the strain life relationship with$(\sigma_f' - \sigma_m)$, where σ_m is the mean stress. A problem is that each different σ_m values generates a different strain life curve. The alternative Smith-Watson-Topper relationship (1970) generates a common curve allowing for different σ_m values. Here the parameter $\sqrt{\sigma_{max}\varepsilon_a E}$ is plotted versus cycles to failure on log-log scales and collapses the data for different levels of mean stress onto a common curve, as shown in Fig. 2. The defect indication specimens which failed show reduced cyclic lives by up to an order of magnitude.

Analysis of Defect Indications

Three methods were employed to establish the nature of the defect indications in the test specimens; scanning electron microscopy (SEM) and energy dispersive X-ray analysis

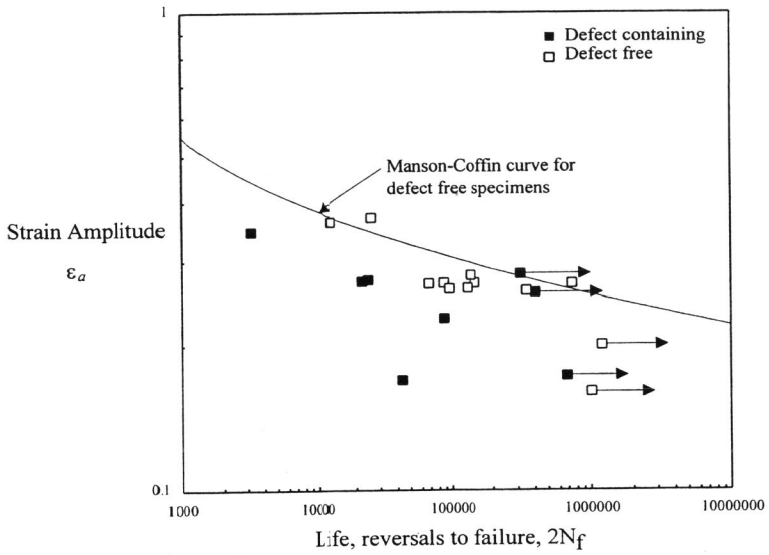

Fig. 1. Strain amplitude versus reversals to failure for defect containing and defect free specimens

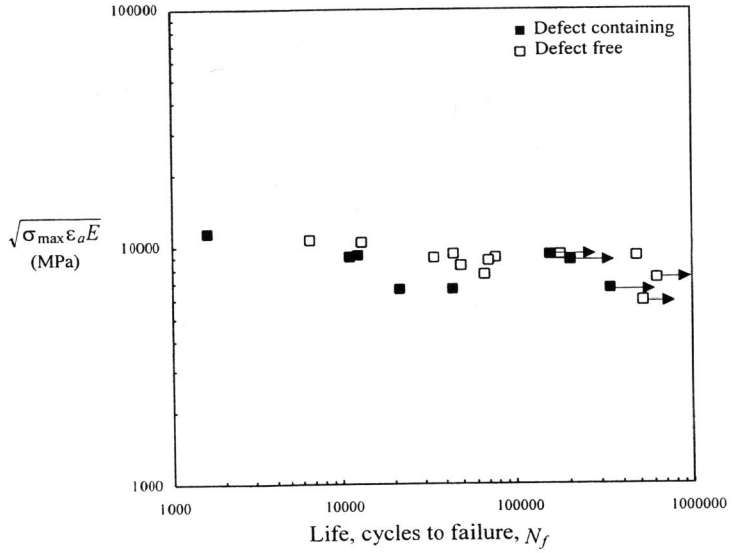

Fig. 2. Smith-Watson-Topper Relationship, $\sqrt{\sigma_{max}\varepsilon_a E}$ versus cycles to failure for defect containing and defect free specimens

(EDS) on fracture surfaces and optical microscopy of polished sections. The NDT indications were found to be due to non-metallic inclusions, with compositions consistent with aluminium and titanium oxides.

An example of a failed defect containing specimen is shown macroscopically in Fig. 3 and in micro-section in Fig. 4. Fatigue cracking was found to have initiated from a cluster of inclusions, and propagated in a trans-granular mode showing typical ductile striations away from the initiation site. The defect specimens giving run out results (arrowed, Fig. 1 & 2) were found to contain only very small clusters of inclusions with dimensions of the order of 0.04 to 0.20 mm. As shown below, even if these defects were taken to be crack-like, their stress intensity range ΔK based on initial size and tensile stress range was below the threshold for crack growth.

Threshold For Fatigue Crack Growth

Optical microscopic examination showed that the initial defect indications were due to clusters of inclusions e.g. see Fig. 4. Values of effective stress intensity range (ΔK_{eff}) based on (i) the initial individual largest defect and (ii) the overall cluster group depth, using the tensile stress range were calculated using the K solution for elliptical cracks due to Pickard,(1986). The values of ΔK_{eff} versus cyclic life are plotted for the individual largest inclusions in Fig. 5 and for the inclusion clusters in Fig. 6.

Table 2. Estimated Defect Size and the Values of Effective Stress Intensity Range, ΔK_{eff}

Inclusions Size (mm)		No. of Cycles to Failure	ΔK_{eff} ($MPa\sqrt{m}$) for Inclusions	
Individual Inclusion	Group of Inclusions		Individual Inclusion	Group of Inclusions
0.02	0.69	51,550	3.67	21.05
0.375	0.375	5,971	22.65	22.65
0.02	0.2	21,552	4.34	13.72
0.01	0.22	337,752*	2.26	3.77
0.01	0.137	12,417	3.05	8.97
0.05	0.05	42,205	4.58	4.58
0.00002	0.389	11,180	0.13	18.65
0.00002	0.1	213,462*	0.12	7.24
0.003	0.04	157,309*	1.64	6
0.04	0.04	43,820	6.56	6.56

(* Failed away from the defect)

The results are compared with the long crack threshold (ΔK_{th}) data of Taghani (1989) for Waspaloy at 600°C (650°C data was not available) at stress ratios between 0.1 and 0.9. It can be seen that all but one of the ΔK_{eff} results based on individual inclusions (Fig. 5) show failure below the long crack ΔK_{th} for R=0.1 at 10.4 $MPa\sqrt{m}$ and all but two failed below the R=0.9 threshold of 4.6 $MPa\sqrt{m}$. However, based on inclusion group size (Fig. 6), a better correlation with the long crack threshold is obtained, particularly if the value of ΔK_{th} at R=0.9 is taken to be the *effective* ΔK_{th}, i.e. closure free, and the better indicator of the threshold for a short crack.

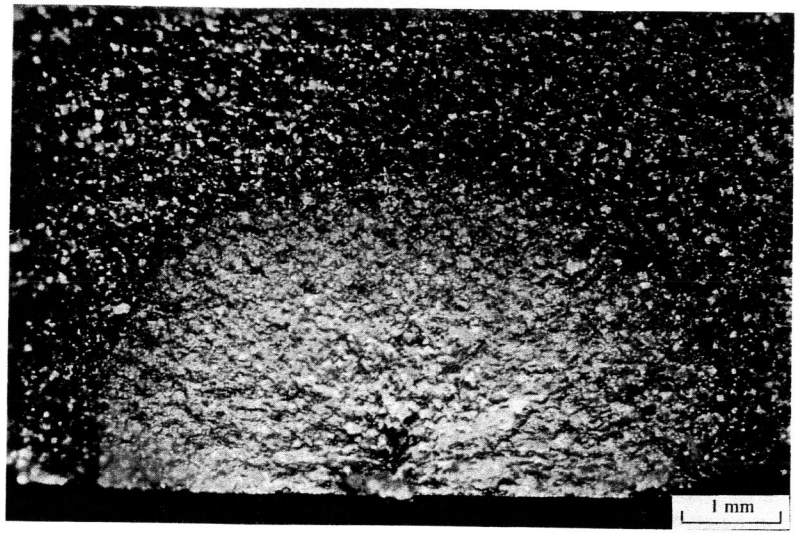

Fig. 3. Fracture surface showing initiation and growth from a sub-surface defect

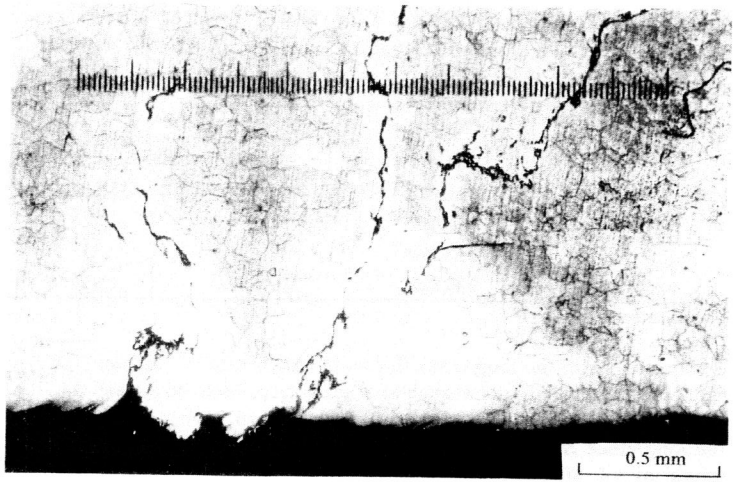

Fig. 4. Micro-section through the crack initiation site showing a cluster of inclusions

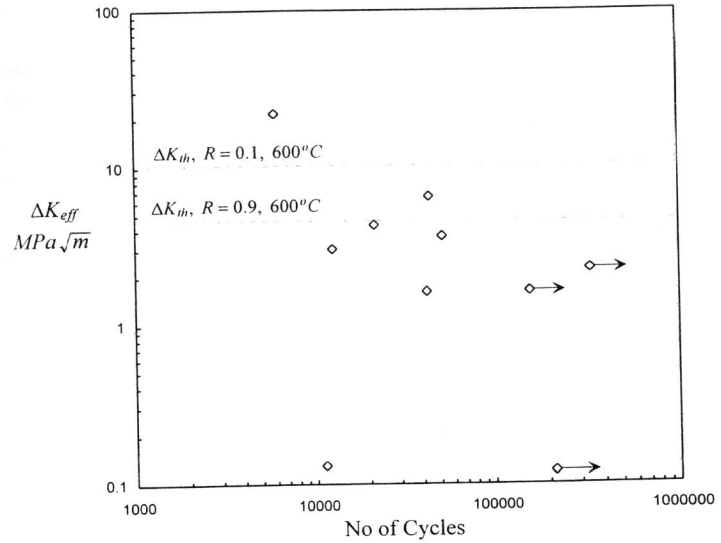

Fig. 5. Initial ΔK_{eff} versus Cycles to Failure, where $\Delta K_{eff} = \Delta K_{tensile}$, calculated from the Minimum Dimension of Individual Inclusions

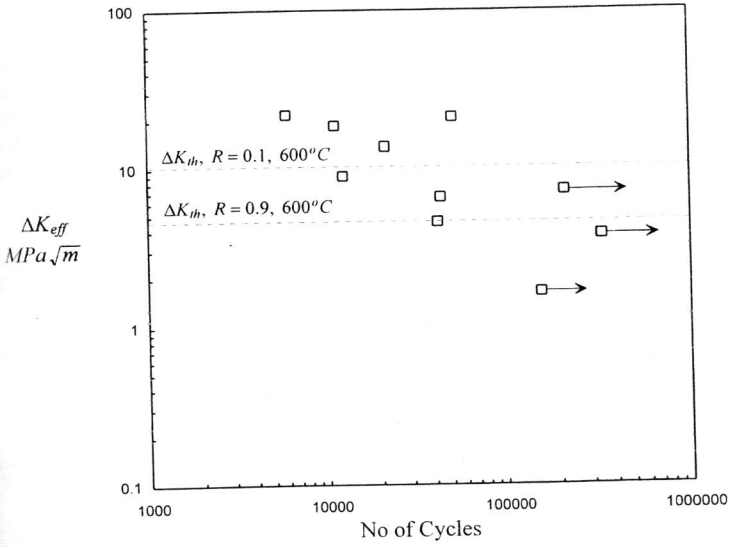

Fig. 6. Initial ΔK_{eff} versus Cycles to Failure, where $\Delta K_{eff} = \Delta K_{tensile}$, calculated from the Depth Dimension of Inclusion Groups

CONCLUSIONS

Fatigue endurance studies have been carried out on Waspaloy at 650°C and 0.25 Hz under load and effective strain control on plane and defect indication specimens with a shot peened surface, to establish the influence of inherent material defects on fatigue life.

In terms of strain life behaviour, the presence of such defect indications is shown to shorten average fatigue lives by about an order of magnitude.

The defect indications were found to be clusters of aluminium and titanium rich oxide inclusions which may act as crack initiation sites, dependent on group size and density.

The use of initial defect cluster size and tensile stress range gives a reasonable ΔK effective versus life correlation, which compares well with the high stress ratio (closure free) threshold for the alloy.

Further study is required to quantity defect nature and behaviour in terms of crack development and propagation in order to establish a fracture mechanics based approach for safe-life prediction.

REFERENCES

Denda, T., P.L. Bretz,and J.K. Tien (1992). Inclusion Size Effect on the Fatigue Crack Propagation Mechanism and Fracture Mechanics of a Superalloy. *Metallurgical Transactions A*, 23A, 519-526.

Jenkins, L.M. and A.C. Pickard (1989). Lifing of Discs. In: *Materials Development in Turbo-Machinery Design* (J.F.Knott and M.H. Lewis ed.), 95-104.

Mitchell, A. (1987). White Spot Defects in VAR Superalloy. *Proc. of Vacuum Metallurgy Conference only Speciality Metals Melting and Processing.* 55-61. Iron and Steel Soc./AIME.

Morrow, J. (1968). In: Fatigue Design Handbook. 21-29. Society of Automotive Engineers.

Pickard,A.C. (1986). In: The Application of 3-Dimensional Finite Element Methods to Fracture Mechanics and Fatigue Life Prediction, 81-116.

Smith,K.N., P. Watson, and T.H. Topper (1970). A Stress-Strain Function for the Fatigue of Metal. *Journal of Materials,* 5 , No. 4. 767-778.

Taghani, N. (1989). Crack Growth in Gas Turbine Alloys due to High Cycle Fatigue. *M.Phil. Thesis (CNAA), University of Portsmouth*, 113.

Tavernelli, J.F. and L.F.Coffin Jr. (1962). Experimental Support for Generalized Equation Predicting Low Cycle Fatigue. *Trans. ASME, J. Basic Eng.* 84, No. 4. 533.

Manson, S.S. (1962). Discussion of above. *Trans. ASME J. Basic Eng.*, 84, No. 4, 537.

Webster, P.S. and T.P. Cunningham (1993). The Application of Shot Peening Technology in the Aero Engine Industry. In: *Shot Peening Techniques and Applications* (K.J.Marsh, ed.), 179-207.

ACKNOWLEDGEMENTS

Joint funding by Rolls-Royce plc and the D.R.A. is gratefully acknowledged.